***IN-SITU* MINERALOGICAL ANALYSIS OF THE VENUS SURFACE USING X-RAY DIFFRACTION AND X-RAY FLUORESCENCE (XRD/XRF).** P. Sarrazin[1], D.F. Blake[2], T.S. Bristow[2], E.B. Rampe[3], A.H. Treiman[4] and K. Zacny[5]. [1]eXaminArt, Mountain View CA (philippe.sarrazin@examinart.com); [2]NASA Ames Research Center, Moffett Field, CA; [3]NASA Johnson Space Center, Houston, TX; [4]Lunar and Planetary Institute, Houston, TX; [5]HoneyBee Robotics, Pasadena, CA.

Introduction: *Quantitative* and *definitive* mineralogy is critical for elucidating the early history and evolution of Venus, for comparative planetology of the rocky planets, for deducing potential habitability on early Venus, and for characterizing Venus as a surrogate for Venus-like exoplanets.

The history of a planet is written in its rocks and the minerals they contain. Because minerals are stable under known ranges of temperature, pressure and composition, a rock comprised of specific minerals can be used to identify the conditions under which it formed and subsequent environmental changes, based on individual mineral stability ranges and the presence or absence of equilibrium between them. XRD/XRF analysis of drilled and powdered Venus regolith can provide:

- Identification of all minerals present >1 wt. %.
- Quantification of all minerals >3 wt. %, including their structure states and cation occupancies.
- Bulk geochemistry of major, minor and some trace elements.
- Abundance of all major elements present in each mineral (H and above).
- Valence state of all elements, including speciation of multi-valent species, such as Fe.
- Abundance and composition of X-ray amorphous components, if present.

The CheMin-V XRD/XRF instrument: CheMin-V is a combined X-ray Diffractometer (XRD, quantitative mineralogy) and X-ray Fluorescence Spectrometer (XRF, quantitative elemental composition) that will analyze powdered samples delivered to it inside the pressure shell of the Venus lander by the HoneyBee Robotics Venus drill [1]. CheMin-V is a next-generation XRD/XRF instrument having MSL-CheMin [2] heritage, augmented by enhanced XRD and XRF capability. Drilled and powdered Venus regolith samples are sieved to <150 µm and delivered to separate XRD and XRF cells for analysis (Fig. 1).

XRD geometry and XRD sample cell description: The collimated X-ray beam from the source is directed through a thin layer (~175 µm) of <150 µm grain size Venus regolith confined between two 8 mm-diameter, 7 µm thick Kapton™ windows in the XRD sample cell (e.g., cell 1A in Fig. 1). The sample cell is shaken causing the loose powder to flow in a convection motion through the beam. The 2-D pattern is summed circumferentially around the central non-diffracted beam to yield a conventional 1-D XRD pattern (Fig 2).

CheMin-V will employ Hybrid Pixel Detectors (HPDs) in place of the single CCD used in MSL-CheMin. HPDs are radiation hard and do not require cooling. An array of 4 HPDs increases the resolution of the instrument from 0.3° to 0.2° 2θ, sufficient to identify and quantify 3-pyroxene systems.

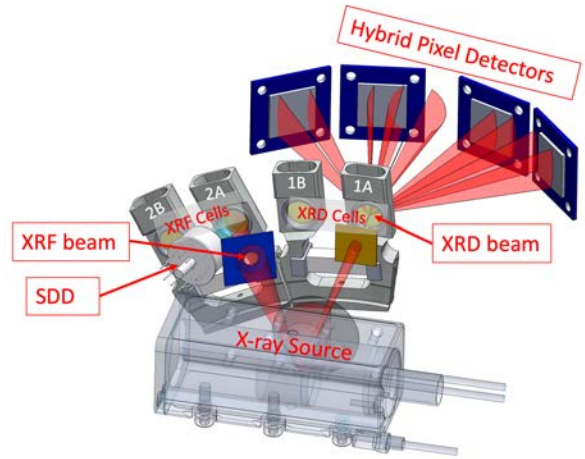

Fig. 1: Geometry of CheMin-V. A single X-ray source emits two separate beams, the first optimized for XRD and the second optimized for XRF.

Fig. 2 shows an XRD pattern of Apollo 14 regolith sample 14149,26 collected in a 1 hour acquisition with a Terra™ XRD [3] (similar XRD geometry to CheMin-V), and quantified using Rietveld refinement [4] and whole pattern fitting [5]. The resulting analysis is shown in Table 1.

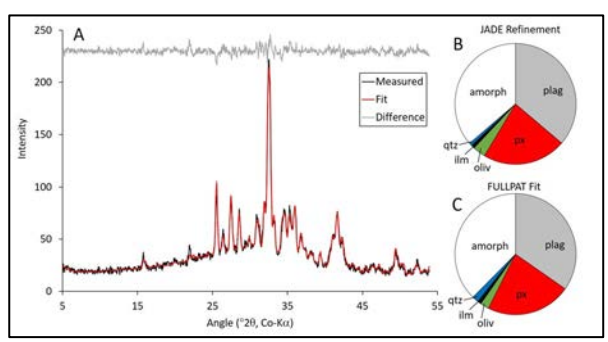

Fig 2: Terra XRD pattern of <150 µm grainsize separate of Apollo 14 regolith sample 14149,26. Inset pie diagrams show proportions of crystalline and amorphous components determined using Rietveld refinement [4] and FULLPAT whole pattern fitting [5].

CheMin-V XRD patterns can be used to discriminate between basaltic and rhyolitic glasses based on the position of the peak maximum of the amorphous hump in the X-ray diffraction pattern and can accurately quantify glass in the regolith if present in sufficient abundance.

Table 1. Phase Abundances and Mineral Compositions in Apollo 14 Regolith 14149,26

Mineral	Abundance[1]	Composition[2]
Plagioclase Feldspar	33.6 (0.8)	$Ca_{0.94(4)}Na_{0.06}Al_{1.94}Si_{2.06}O_8$
Augite	7.1 (0.6)	$Mg_{0.54(23)}Ca_{0.63(11)}Fe_{0.83(25)}Si_2O_6$
Orthopyroxene	8.5 (0.7)	$Mg_{1.27(6)}Fe_{0.61(6)}Ca_{0.12(2)}Si_2O_6$
Pigeonite	7.3 (0.7)	$Mg_{1.26(20)}Fe_{0.53(21)}Ca_{0.21(7)}Si_2O_6$
Olivine	3.5 (0.4)	$Mg_{1.46(10)}Fe_{0.54}SiO_4$
Quartz	0.9 (0.1)	SiO_2
Ilmenite	1.0 (0.2)	$FeTiO_3$
X-ray Amorphous	38.0 (6.0)	in combination with XRF data[3]
Total	99.7	

[1]Values in parentheses are 1σ errors. [2]Calculated from unit-cell parameters [6] refined using MDI-JADE™. [3]The composition of the X-ray amorphous component can be determined by subtracting the composition of the crystalline component (derived from unit cell parameters) from the bulk XRF composition.

XRF geometry and sample cell description: A divergent X-ray beam from the source fluoresces the active volume of the XRF sample cell (e.g., cell 2A in Fig. 1) which is 8 mm in diameter and 3 mm thick. The front window of the cell is made of an 8 mm-diameter, 4 µm-thick beryllium foil and the back window is made of an 8 mm-diameter Pt disc that is sufficiently thick to block X-ray transmission. XRF data are collected with a silicon drift detector (SDD) placed in reflection geometry (Fig. 1).

Predicted XRF performance of CheMin-V: Fundamental Parameters calculations [7] and Monte Carlo methods [8] were used to model the XRF performance of CheMin-V. Table 2 shows the calculated quantification and detection limits for select major, minor and trace elements in a basaltic or rhyolitic matrix.

The Advantage of Hybrid Detectors for XRD: CCD detectors require deep-cooling and must operate under single photon counting conditions which limit X-ray flux. Hybrid Pixel Detectors do not require cooling and can operate under high flux conditions (Fig 3). These detectors will replace CCDs in all future XRD instruments developed by our group. In a configuration like Fig. 1, this results in decreased analysis times, increased 2θ resolution and improved XRF performance along with much reduced power requirements.

Discussion: CheMin-V meets or exceeds the requirements of six investigations described in the "Scientific Goals, Objectives and Investigations for Venus Exploration" document [9] that pertain to measurements of Venus surface chemistry and mineralogy: I. A. Hydrous Origins (1); I. A. Reycling (1); III. A. Geochemistry (1); III. B. Local Weathering (1); III. B. Global Weathering (2); and III. B. Chemical Interactions (3). XRD and XRF are listed as payload elements of the Venus Flagship Lander in the 2023-2032 Planetary Decadal Survey report [10].

Table 2. Quantification & Detection Limits in Basaltic or Rhyolitic Matrices Using XRF[1,2]

(Major Elements)			
Z	Element	Quant. Limit (µg/g)	Det. Limit (µg/g)
11	Na	592	178
12	Mg	239	72
13	Al	117	36
14	Si	86	26
15	P	72	22
16	S	28	9
17	Cl	21	7
19	K	6	2
20	Ca	7	2
22	Ti	6	2
24	Cr	3	1
25	Mn	2	1
26	Fe	8	3

(Zr, Selected REE and Th)			
Z	Element	Quant. Limit (µg/g)	Det. Limit (µg/g)
40	Zr	10	3
57	La	10	3
58	Ce	15	5
60	Nd	6	2
62	Sm	5	2
63	Eu	51	16
64	Gd	42	13
66	Dy	119	36
68	Er	158	48
70	Yb	25	8
71	Lu	24	7
90	Th	17	5

[1] Based on 1 hour of analysis
[2] These are "best case" values that do not take into account peak interferences. "Real world" detection and quantification limits in some cases will be higher, as for example Na or Mg in the presence of abundant Al.

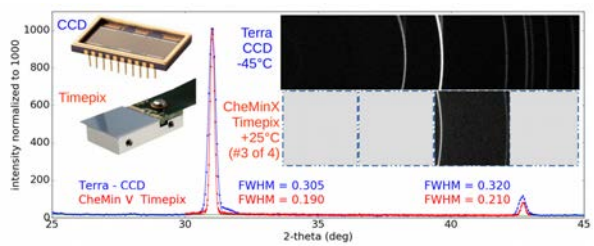

Fig 3: Comparison of XRD data of quartz using a CCD based Terra [3] vs. a HPD detector placed twice as far from the sample. HPDs do not require cooling, while the CCD must be hermetically sealed in a chamber and cooled to -45C. This preliminary measurement verifies the much improved resolution of CheMinX.

Acknowledgments: This work was made possible by support from NASA's DALI (#18-DALI18_2-0006) and MatISSE (#16-MATISE16_2-0005) programs to DFB.

References: [1] Zacny et al. (2014), *IEEE Aerospace Conference*, 3-7 March, Big Sky MT. [2] Blake et al. (2012), *Space Sci. Rev.,* **170**, 341-478, 10.1007/s11214-012-9905-1. [3] Sarrazin et al. (2008), *LPSC* **39**, #2421. [4] Bish & Post (1993), *Am. Min.* **78**, 932–942. [5] Chipera & Bish (2002), *J. App. Cryst.*, **35**, 744-749. [6] Morrison et al., (2018), *Am. Min,*. 10.2138/am-2018-6123. [7] Sole´ et al, 2007), *Spectrochim. Acta Part B,* ***62***, 63-68. [8] Schoonjans et al. (2012) *Spectrachim. Acta Part B, 70*, 10-23. [9] GOI for Venus Exploration (2019). [10] Planetary Decadal Survey 2023-2032, p. C12.